Received: 24 May 2023 | Revised: 20 December 2023 | Accepted: 22 December 2023

DOI: 10.1002/bit.28652

ARTICLE

BIOTECHNOLOGY AND BIOENGINEERING WILEY

A novel experimental method to determine substrate uptake kinetics of gaseous substrates applied to the carbon monoxide-fermenting *Clostridium autoethanogenum*

Maximilienne T. Allaart[1] | Charilaos Korkontzelos[1] | Diana Z. Sousa[2] | Robbert Kleerebezem[1]

[1]Department of Biotechnology, Delft University of Technology, Delft, The Netherlands

[2]Laboratory of Microbiology, Wageningen University & Research, Wageningen, Netherlands

Correspondence
Robbert Kleerebezem, Department of Biotechnology, Delft University of Technology, Delft, The Netherlands.
Email: r.kleerebezem@tudelft.nl

Funding information
Nederlandse Organisatie voor Wetenschappelijk Onderzoek

Abstract

Syngas fermentation has gained momentum over the last decades. The cost-efficient design of industrial-scale bioprocesses is highly dependent on quantitative microbial growth data. Kinetic and stoichiometric models for syngas-converting microbes exist, but accurate experimental validation of the derived parameters is lacking. Here, we describe a novel experimental approach for measuring substrate uptake kinetics of gas-fermenting microbes using the model microorganism *Clostridium autoethanogenum*. One-hour disturbances of a steady-state chemostat bioreactor with increased CO partial pressures (up to 1.2 bar) allowed for measurement of biomass-specific CO uptake- and CO_2 production rates (q_{CO}, q_{CO_2}) using off-gas analysis. At a p_{CO} of 1.2 bar, a q_{CO} of -119 ± 1 mmol g^{-1}_X h^{-1} was measured. This value is 1.8–3.5-fold higher than previously reported experimental and kinetic modeling results for syngas fermenters. Analysis of the catabolic flux distribution reveals a metabolic shift towards ethanol production at the expense of acetate at $p_{CO} \geq 0.6$ atm, likely to be mediated by acetate availability and cellular redox state. We characterized this metabolic shift as acetogenic overflow metabolism. These results provide key mechanistic understanding of the factors steering the product spectrum of CO fermentation in *C. autoethanogenum* and emphasize the importance of dedicated experimental validation of kinetic parameters.

KEYWORDS
acetogen, chemostat, metabolic shift, overflow metabolism, pulse feeding, syngas

1 | INTRODUCTION

One of the most critical challenges of our society today is to transition effectively from a petrol-based to a circular economy. Reaching a circular economy requires waste streams to be perceived as resources. Gasification provides an avenue for reusing recalcitrant or non-biodegradable waste streams and yields carbon monoxide (CO)-rich syngas (Arena, 2012). CO is a carbon and energy source that can be (biologically) assimilated into chemical building blocks. Another CO-rich waste stream is flue gas, which originates from steel

processing (Molitor et al., 2016). This gas is currently detoxified by combustion, leading to approximately 3.9 billion tonnes of CO_2 emissions per year (IEA, 2020; World Steel Organization, 2022). Thus, for the transition to a bio-based society, a robust technology for the conversion of CO into chemical building blocks is needed.

Purely chemical gas conversion processes such as Fischer–Tropsch synthesis are sensitive to gas composition and impurities (Dry, 2002). Therefore, novel technologies for syngas and flue gas conversion must be developed. Anaerobic acetogenic microorganisms are known to convert syngas constituents into products such as acetate and ethanol (Abrini et al., 1994; Arantes et al., 2020; Lee et al., 2019; Levy et al., 1981). These organisms are less sensitive to changes in gas composition than metal catalysts and can withstand the presence of impurities like NH_3 and H_2S (Ahmed & Lewis, 2007; Klask et al., 2020; Rückel et al., 2021). Additionally, processes with microbial catalysts are less energy-demanding because they can be operated at mild temperatures and pressures. Microbial conversions, therefore, provide interesting opportunities for valorizing CO-rich gases (de Lima et al., 2022; Heffernan et al., 2020; Molitor et al., 2016; Valgepea et al., 2018).

It is crucial to have a thorough understanding of the kinetics of microbial conversions for the design of large-scale CO fermentation processes (Wett et al., 2007). However, there is currently a lack of kinetic information related specifically to syngas fermentation (Heffernan et al., 2022). This knowledge gap is likely related to the difficulty of accurately measuring substrate concentrations, as both gas-liquid mass transfer of poorly soluble CO and microbial uptake rates govern the substrate concentration in the broth. Consequently, classical batch bottle incubations are inadequate for the kinetic characterization of gas fermenting microbes (Sipkema et al., 1998). Therefore, previously reported kinetic parameters obtained in batch bottle experiments (Mohammadi et al., 2014) are untrustworthy, as it is highly challenging to determine whether the observed rates were limited by mass transfer, biological capacity, or inhibited by carbon monoxide from the available data. Furthermore, the pH, biomass-, substrate-, and product concentrations are not constant over time in batch bottle incubations. All these factors affect gas–liquid mass transfer properties, which in turn influence CO availability (Cotter et al., 2009; Puiman et al., 2022).

Some of these limitations are overcome when using chemostat cultivation in bioreactors. Mathematical modeling studies using steady-state chemostat data for kinetic parameter estimation have also been conducted. Such studies estimated maximum biomass-specific CO uptake rates (q_{CO}^{max}) between −37.5 and −46.3 mmol g_X^{-1} h^{-1} for different closely related *Clostridium* strains (de Medeiros et al., 2019). More recently, however, experimental data was published in which a much higher q_{CO} of approximately −70 mmol g_X^{-1} h^{-1} was sustained during chemostat operation (de Lima et al., 2022). These variations between model predictions and new experimental observations highlight the significant influence of input data on kinetic parameter estimation. Therefore, gas-fermenting microbes should not only be cultivated in chemostats, but also in dynamic environments to improve the verification of kinetic model parameters. Bioreactors with controllable gas-liquid mass transfer properties and online off-gas analysis are highly suitable for assessing the substrate uptake capacity of gas fermenting organisms (Novak et al., 2021). However, parameter estimation through dynamic cultivation approaches still requires careful experimental design. Useful kinetic models often include many parameters, which must be identified in different experiments. Given the significant disparity between modeling and experimental results for CO uptake rates in recent literature, this study focuses on one of the essential kinetic parameters, q_{CO}^{max}, of *Clostridium autoethanogenum* in dynamic bioreactor experiments.

We used CO-grown chemostat cultures to study the CO uptake kinetics of *C. autoethanogenum*. We exposed them to pulses of increasing CO partial pressures (p_{CO}) to identify the maximum substrate uptake rate. The pulse experiments were carried out for one hour to prevent significant growth of the microorganism. In this way, we assessed the immediate capacity of the microorganism to consume CO, circumventing the need to reach a different steady state at increased CO supply.

2 | MATERIALS AND METHODS

2.1 | Cultivation media and pre-culturing

C. autoethanogenum DSM10061 was obtained from colleagues at Wageningen University as an anaerobic pre-culture grown on fructose. Routine batch bottle cultivation was done in 100 mL serum bottles with a working volume of 50 mL. The mineral medium contained 0.9 g NH_4Cl, 0.9 g NaCl, 0.2 g $MgSO_4 \times 7H_2O$, 0.75 g KH_2PO_4, 1.5 g K_2HPO_4, 0.02 g $CaCl_2 \times 2H_2O$, 0.5 mg Na-resazurin, 1 mL of SL-10 trace elements and 0.2 mL of alkaline trace elements per liter. The SL-10 trace elements solution contained (in g L^{-1}): $FeCl_2 \times 4\ H_2O$ 1.5, $FeCl_3 \times 6\ H_2O$ 2.5, $ZnCl_2$ 0.07, $MnCl_2 \times 4\ H_2O$ 0.1, H_3BO_3 0.006, $CoCl_2 \times 6\ H_2O$ 0.19, $CuCl_2 \times 2\ H_2O$ 0.002, $NiCl_2 \times 6\ H_2O$ 0.024, $Na_2MoO_4 \times 2\ H_2O$ 0.036, and 10 mL 25% HCl. The alkaline trace elements solution contained (in g L^{-1}): NaOH 0.4, Na_2SeO3 0.017, $Na_2WO_4 \times 2\ H_2O$ 1.03, $Na_2MoO_4 \times 2H_2O$ 0.024. After autoclaving, the headspace was exchanged with 100% CO and the headspace pressure was set to 1.5 bar. Before inoculation yeast extract (0.5 g L^{-1}), B vitamins (2 mL L^{-1}), and L-cysteine-HCl × H_2O (0.75 g L^{-1}) were added from sterile stock solutions. The B vitamin solution contained (in g L^{-1}): biotin 0.02, nicotinamide 0.2, p-aminobenzoic acid 0.1, thiamine hydrochloride 0.2, Ca-pantothenate 0.1, pyridoxamine 0.5, cyanocobalamin 0.1, and riboflavin 0.1.

Bioreactor cultivation was done using a chemically defined medium without yeast extract as described by Valgepea et al. (2017). The mineral medium contained per liter: 0.5 g $MgSO4 \times 6H_2O$, 0.2 g NaCl, 0.1 g $CaCl_2$, 2.65 g $NaH_2PO_4 \times 2H_2O$, 0.5 g KCl, 2.5 g NH_4Cl, 0.017 g $FeCl_3 \times 6H_2O$, 0.5 mg Na-resazurin, 10 mL trace metal solution (TMS). The TMS contained per liter: 1.5 g trisodium nitrilotriacetate, 3 g $MgSO_4 \times 7H_2O$, 0.5 g $MnSO_4 \times H_2O$, 1 g NaCl,

0.667 g $FeSO_4 \times 7H_2O$, 0.2 g $CoCl_2 \times 6H_2O$, 0.2 g $ZnSO_4 \times 7H_2O$, 0.02 g $CuCl_2 \times 2H_2O$, 0.014 g $Al_2(SO_4)_3 \times 18H_2O$, 0.3 g H_3BO_3, 0.03 g $NaMoO_4 \times 2H_2O$, 0.02 g Na2SeO$_3$, 0.02 g $NiCl_2 \times 6H_2O$ and 0.02 g $Na_2WO_4 \times 2H_2O$. After sterilizing the medium at 121°C, it was stirred and sparged with N_2 for at least 24 h to strip out the oxygen. Next, 0.5 g L^{-1} of sterile L-cysteine-HCl × H_2O and 2 mL L^{-1} concentrated filter-sterilized vitamin solution were added. The B-vitamin solution contained per liter: 100 mg biotin, 100 mg folic acid, 50 mg pyridoxine hydrochloride, 250 mg thiamine-HCl × H_2O, 250 mg riboflavin, 250 mg nicotinic acid, 250 mg calcium pantothenate, 250 mg cyanocobalamin, 250 mg 4-aminobenzoic acid, and 250 mg thioctic acid. Moreover, 0.5 mL of 37% HCl was added per liter of medium to maintain sterility after cysteine and vitamin addition.

2.2 | Chemostat cultivation

Chemostat cultivation was done in a glass jacketed 3 L bioreactor (Applikon) with a working volume of 1.6 L. The bioreactor was inoculated with 100 mL of exponentially growing *C. autoethanogenum* culture (grown in batch bottles on CO in medium containing yeast extract). CO supply was increased by increasing the stirring speed, gas flow rate, and inlet gas composition until steady-state operational setpoints were reached. After reaching this, in- and effluent pumps were turned on to feed the reactor with a chemically defined medium and control the dilution rate at 0.01 h^{-1}. The gas composition and sparging rate were controlled using separate mass flow controllers for CO and N_2 (Brooks Instruments). The total gas flow rate was kept at 100 mL min^{-1} at 1.0 atm, and the reactor was fed with a 90%/10% mixture of N_2 and CO, respectively, during steady-state operation. The reactor was continuously agitated at a speed of 600 rpm using two equally spaced six-bladed mechanical stirrers, and pH was maintained at 5.5 ± 0.05 using 2 mol L^{-1} NaOH (Applikon InControl). The reactor temperature was maintained at 37°C using a water jacket and a thermostat bath (E300; Lauda). The off-gas was cooled using a cryostat set to 4.5°C to prevent culture broth evaporation.

2.3 | k_La determination

The gas–liquid mass transfer capacity of the bioreactor was assessed at different stirring speeds using a dynamic method. Briefly, this method is based on measuring the concentration of dissolved oxygen in the medium using a dissolved oxygen (DO) sensor (Mettler Toledo). Initially, oxygen was stripped out from the reactor by sparging with N_2 until DO = 0%. Then, air was supplied until oxygen saturation in the medium was reached. The saturation curve was linearized by taking its natural logarithm, and the slope of the obtained curve represented the k_La. After determining the k_La for oxygen, the respective parameter was recalculated for carbon monoxide using the diffusion coefficients of the two gases (2.03×10^{-5} cm^2 s^{-1} for CO and 2.0×10^{-5} cm^2 s^{-1} for O_2. This procedure was performed in duplicates for five different stirring speeds (300, 500, 600, 700, and 800 rpm) in a 3 L bioreactor at 37°C and a gas flow rate of 100 mL min^{-1}. The working volume was 2 L. During the 800 rpm test, excessive foaming occurred. Therefore, a working of 1.6 L was used during chemostat operation.

2.4 | CO pulse experiments

CO pulse experiments were carried out after a steady state was reached in the chemostat. Due to a technical disturbance, experiments were conducted starting from two highly similar steady states (Steady State I and II). A two-sample *t*-test was performed to determine whether the difference between the average biomass concentrations in the two stages was statistically significant. The means and standard deviations of the biomass concentrations are presented in Table 2. Steady State I was maintained for a longer duration than Steady State II, resulting in sample sizes of 89 and 6, respectively.

C. autoethanogenum was subjected to increased p_{CO} for 1 h by increasing the CO concentration in the inlet gas without changing the overall gas supply rate. pCO was increased with 0.05 atm increments up to pCO = 1.0 atm and with 0.1 atm increments up to pCO = 1.2 atm (Table 1). Pulse experiments up to pCO = 0.85 atm were carried out during Steady State I, and of the four pulses at pCO = 0.9 atm. The rest of the pulse experiments were carried out after reaching Steady State II. After 1 h the inlet gas concentration was returned to the original settings (p_{CO} = 0.1 atm). The duration of the pulses was set to 1 h to prevent significant differences in biomass concentration between the start and the end of the pulse. Shorter pulses of 30 min were not sufficient to obtain the stable off-gas profiles required for the calculation of q_{CO}. Limiting biomass growth during the pulses allowed us to use the steady-state biomass concentration to calculate the biomass-specific CO uptake rates during the pulses. pH control was switched off during the pulse experiments to prevent influencing the off-gas measurements. Pulse experiments were carried out in biological duplicates, triplicates, or quadruplicates. Liquid samples were taken either right after termination of the pulse experiment (pulses of 80% CO and above) or when the off-gas measurements returned to the steady-state values. The optical density of the broth was measured to assess whether significant growth had taken place during the pulse experiment. If the optical density increased more than 5% compared with the steady-state value during a pulse experiment, the chemostat was left undisturbed for at least a day before administering the next pulse. The OD never increased more than 10% during a single pulse experiment, validating the use of the steady-state biomass concentration for the calculation of the biomass-specific substrate uptake rate.

2.5 | Analytical methods

The off-gas composition of gas fermentation experiments was followed using an X-stream Enhanced XEGP Off-Gas Analyzer equipped with an

TABLE 1 Conditions during pulse experimentation.

p_{CO} [atm]	CO flow [mL min^{-1}]	N_2 flow inlet [mL min^{-1}]	N_2 flow off-gas [mL min^{-1}]	Headspace overpressure [atm]	Number of replicates [−]
0.15	15	85	0	-	4
0.20	20	80	0	-	4
0.25	25	75	0	-	4
0.30	30	70	0	-	4
0.35	35	65	0	-	4
0.40	40	60	0	-	4
0.45	45	55	0	-	4
0.50	50	50	0	-	4
0.55	55	45	0	-	3
0.60	60	40	100	-	3
0.65	65	35	100	-	4
0.70	70	30	100	-	2
0.75	75	25	100	-	3
0.80	80	20	100	-	3
0.85	85	15	100	-	3
0.90	90	10	100	-	4
0.95	95	5	100	-	2
1.00	100	0	100	-	3
1.10	100	0	100	0.1	2
1.20	100	0	100	0.2	2

Note: To maintain a constant inlet gas flow rate ($F_{G,\ in}$) of 100 mL min^{-1} a supply of N_2 was introduced. Additionally, an N_2 flow in the off-gas was used to dilute the bioreactor off-gas to values within the measuring range of the off-gas analyzer.

infrared detector for CO and CO_2 (6 mm and 30 mm, respectively) measurement and a thermal conductivity detector for H_2 measurement (Emerson). During pulse experiments with an inlet gas fraction of CO above 60%, the off-gas was diluted with 100 mL min^{-1} N_2 gas to stay within the measuring range of the off-gas analyzer.

Biomass concentrations were monitored by measuring optical density (OD_{660}) and the amount of VSS in the broth using 100 mL effluent (APHA/AWWA/WEF, 1999). Both OD and VSS were always determined in duplicate. OD and VSS correlated linearly (VSS = 0.2935 × OD_{660}). Acetate, lactate, formate, 2,3-butanediol, and ethanol concentrations were determined using a Vanquish (Thermo Fisher Scientific) high-performance liquid chromatography machine (HPLC) with an Aminex HPX-87H column (BioRad) at 50°C coupled to a refractive index- and ultraviolet detector (Waters). 1.5 mmol L^{-1} phosphoric acid was used as eluent at 0.75 mL min^{-1}. Biomass was removed from the reactor samples before storage or measuring fermentation products by filtration using a 0.22 µm membrane filter (Millipore, Millex-GV).

2.6 | Determination of biomass-specific CO uptake and CO_2 production rates

The calculation of q_{CO} and q_{CO_2} was conducted from the data gathered in the last 10 min of the CO pulse. During this time frame, the gas profile was stable and reflected the biological consumption of CO. The first 50 min of the experiment were excluded from calculations, as the gradual increase in CO measured in the off-gas in this period is a result of incomplete gas mixing in the headspace of the reactor (Supporting Information: Figure S1).

CO consumption leads to the production of acetate, ethanol, and CO_2 via the following two stoichiometries:

$$4CO + 2H_2O \rightarrow \text{Acetate} + 2CO_2 \quad (1)$$

$$6CO + 3H_2O \rightarrow \text{Ethanol} + 4CO_2 \quad (2)$$

CO uptake and CO_2 production were calculated using gas- and liquid mass balances. First, the volumetric outflow of the reactor was calculated using the inert fraction (N_2) of the inlet gas as reference, assuming the gas phase was in steady state in the last 10 min of the pulse experiment:

$$\frac{dN_{N_2}}{dt} = F_{G,in}\, y_{in,N_2} - F_{G,out}\, y_{out,N_2} \quad (3)$$

$$y_{out,N_2} = 1 - y_{out,CO} - y_{out,CO_2} - y_{out,H_2} \quad (4)$$

For CO and CO_2 in the gas phase, mass transfer to and from the liquid, respectively, must be considered:

$$\frac{dN_i}{dt} = F_{G,in}\, y_{in,i} - F_{G,out}\, y_{out,i} \pm T_{N,i} \quad (5)$$

The general mass balance equation for a species in the liquid is as follows:

$$\frac{dM_i}{dt} = F_{L,in} C_{in,i} - F_{L,out} C_{out,i} + T_{N,i} + q_i C_x V_L \quad (6)$$

For CO, this equation can be simplified under the assumption that the in-and outflowing liquids contain negligible concentrations of CO:

$$\frac{dM_{CO}}{dt} = T_{N,CO} + q_{CO} C_x V_L \quad (7)$$

When stable off-gas values were measured during a pulse experiment, pseudo-steady state was assumed for CO, due to which the $\frac{dM_{CO}}{dt}$ – term becomes zero. As CO is consumed, the value of q_{CO} will become negative.

CO_2 has a higher solubility than CO, so the concentration in the outflowing liquid must be taken into account. The inflow concentration of CO_2 is negligible as the medium does not contain (bi) carbonate. All soluble CO_2 species (H_2CO_3, HCO_3^-, CO_3^{2-}) are included in the CO_2 terms in the balance equation to calculate the biomass-specific CO_2 production rate:

$$\frac{dM_{CO_2}}{dt} = -F_{L,out}C_{out,CO_2} + T_{N,CO_2} + q_{CO_2}C_x V_L. \quad (8)$$

CO_2 speciation is strongly affected by the increasing CO_2 partial pressure and the increasing pH during a CO pulse. Therefore, dissolved concentrations of CO_2 species (H_2CO_3, HCO_3^-, CO_3^{2-}) were calculated at each collected data point (1-min intervals). It was assumed that the gas and liquid phase were in equilibrium at each data point. The dissolved inorganic carbon concentration was calculated using the equilibrium constants for the different CO_2 species at 37°C as a function of the off-gas partial pressure and pH. The equilibrium assumption was verified by estimating the mass transfer rate in the bioreactor ($k_L a$) from the pulse data and the dissolved CO_2 concentration required for the observed transfer rate. This concentration differed less than 10% from the maximum equilibrium concentration of CO_2, confirming that assuming equilibrium for the inorganic carbon species in the system was valid. The increase in total CO_2-equivalents in the liquid was calculated through integration over the timespan of the pulse and used to correct the observed q_{CO2} from the off-gas measurements.

2.7 | Flux distribution analysis

Assuming the carbon flux to biomass is negligible, the product spectrum of syngas fermentation can be inferred directly from the off-gas measurements. All carbon and electrons that enter the cell must be recovered in the products. The compounds considered were CO, H_2, CO_2, acetate, and ethanol. 2,3-BDO production was neglected as this was never produced in quantifiable amounts in this study. Then, two balance equations describe the microbial conversion (Equations 7, 8). Three of the stoichiometric coefficients are needed as input, and the other two can be calculated. Here, CO, H_2, and CO_2 are used as inputs, as they are continuously measured, to calculate ethanol and acetate. All fluxes are defined as positive, considering CO and H_2 as substrates and CO_2, acetate, and ethanol as products. Since there is a stoichiometric coupling between substrates and products, biomass-specific rates can also be used as input to calculate the production rates. In that case, $v_i = q_i$. The MATLAB script for flux distribution analysis can be found here: https://data.4tu.nl/private_datasets/6gzFKW_nNWmOXB0eypwsUGa6YTm1LNpIYaV7BFrx5XQ

The balance equations for carbon and electrons (with inorganic carbon as reference oxidation state) are:

$$\frac{dC}{dt} = v_{CO} - v_{CO_2} - 2v_{Ac} - 2v_{EtOH}, \quad (9)$$

$$\frac{de^-}{dt} = 2v_{CO} + 2v_{H_2} - 8v_{Ac} - 12v_{EtOH}. \quad (10)$$

In addition to the distribution of excreted products, we calculated the flux distribution over key catabolic reactions to assess the effect of different feeding regimes on the energy conservation of the microorganism. With the biochemistry represented in Supporting Information S1: Figure S6, a script of intracellular balance equations was written in MATLAB R2020a to calculate the intracellular distribution of carbon and electrons, given a specific stoichiometry of CO, CO_2, and H_2. This was done using all steps of the catabolism that use redox carriers (NAD(H), NADP(H), Fd($^{2-}$)). For a feasible overall stoichiometry, each electron carrier's oxidation and reduction must be balanced. This led to the derivation of the redox carrier balances, with the enzyme abbreviations as used in Supporting Information: Figure S6:

$$\frac{dFd^{2-}}{dt} = v_{CODH} + 0.5v_{H_2} + v_{MTHFR} - v_{Rnf} - v_{AOR} - v_{Nfn} - 0.5v_{FDH} - v_{CODH/ACS} \quad (11)$$

$$\frac{dNADH}{dt} = v_{Rnf} + v_{ALDH} - 2v_{MTHFR} - v_{ADH} - v_{Nfn} \quad (12)$$

$$\frac{dNADPH}{dt} = 0.5v_{H_2} + 2v_{Nfn} - v_{MTHFD} - 2v_{FDH} \quad (13)$$

In this model, we assumed that all CO entering the cell is oxidized upon generation of reduced ferredoxin ($v_{CO} = v_{CODH}$). To be able to solve the system, it was constrained so that no metabolites could accumulate intracellularly and that all ATP invested in the methyl branch of the Wood–Ljungdahl pathway (WLP) was recuperated in the acetate kinase reaction. Lastly, an additional flux for acetate excretion (with no additional costs) was added as acetate can either be excreted or further reduced to acetaldehyde and ethanol.

The constraints were formulated as:

$$v_{FDH} = v_{MTHFD} \quad (14)$$

$$v_{MTHFD} = v_{MTHFR} \quad (15)$$

$$v_{CODH/ACS} = v_{FDH} \quad (16)$$

$$v_{ACK} = v_{Ac} + v_{AOR} \quad (17)$$

$$v_{AOR} = v_{ALDH} + v_{ADH} \quad (18)$$

$$v_{MTHFD} = v_{ACK} \quad (19)$$

This system of equations was solved using a least-squares nonlinear solver. The system proved to be robust: it was not sensitive to changes in initial values, and the solution space did not have to be constrained for a correct solution to be obtained.

The biomass-specific ATP production rate (q_{ATP}) was calculated in steady-state by multiplying q_{Rnf} with the assumed H^+/ATP stoichiometry of *C. autoethanogenum* (Supporting Information: Figure S6). Dividing the imposed steady-state growth rate in the chemostat ($\mu = 0.01\ h^{-1}$) by q_{ATP} gives the molar growth yield on ATP (Y_{ATP}) (Stouthamer & Bettenhaussen, 1973). Assuming that Y_{ATP} stays constant over the range of tested p_{CO}, the growth rate during a CO pulse was calculated by multiplying q_{ATP} with Y_{ATP}.

3 | RESULTS

3.1 | Steady-state chemostat operation

C. autoethanogenum was cultivated in a chemostat with a working volume of 1.6 L at a dilution rate of 0.01 h^{-1} and sparged with 100 mL min^{-1} of 10% CO and 90% N_2 gas. Steady state was assumed when stable off-gas, biomass, and product concentrations were measured for at least two liquid volume exchanges. During CO pulse experiments, steady state was disturbed once due to technical problems. After restarting the system, a new steady state was reached, though with a statistically different ($p < 0.05$) biomass concentration (0.52 ± 0.02 and 0.59 ± 0.03 g L^{-1} for Steady Stages 1 and 2, respectively). Slight differences in broth composition can affect the mass transfer rates in bioreactor systems (Puiman et al., 2022b), which could have caused the slight differences in biomass concentrations in the different steady states. As the biomass concentration is used to calculate q_{CO}, the results for the two different steady states are reported separately (Table 2). Both steady states were characterized by a q_{CO} of approximately −10 mmol g_x^{-1} h^{-1} and a q_{CO_2} of approximately 6.2 mmol g_x^{-1} h^{-1}. The liquid product spectrum consisted of acetate and small amounts of ethanol.

TABLE 2 Biological CO consumption and product formation rates, and corresponding biomass concentrations in steady state chemostats.

	Steady State I	Steady State II
q_{CO} [mmol·g_x^{-1}·h^{-1}]	−10.80 ± 0.54	−9.85 ± 0.46
q_{CO_2} [mmol·g_x^{-1}·h^{-1}]	6.26 ± 0.35	6.16 ± 0.76
$q_{Acetate}$ [mmol·g_x^{-1}·h^{-1}]	1.86 ± 0.29	1.82 + 0.09
$q_{Ethanol}$ [mmol·g_x^{-1}·h^{-1}]	0.21 ± 0.04	0.16 ± 0.02
C_x [g_x·L^{-1}]	0.52 ± 0.02	0.59 ± 0.03

Note: Following the resolution of a technical operation issue, Steady State II was obtained in the same bioreactor under identical operational conditions as Steady State I. Standard deviations were calculated from gas- and liquid measurements before the steady state was disturbed with CO pulses.

3.2 | Biological CO uptake increases linearly with increasing CO partial pressures

To assess the CO uptake capacity of *C. autoethanogenum*, the CO concentration in the inlet gas was increased for 1 h. The maximum rate of CO uptake depends on the mass transfer rate, which was manipulated by adjusting the inlet partial pressure of CO and the headspace pressure (Table 1).

Figure 1 shows a clear linear correlation between p_{CO} in the inlet gas and q_{CO} and q_{CO_2}. It was observed that q_{CO} decreased up to −119 ± 1 mmol g_x^{-1} h^{-1} with increasing p_{CO}. q_{CO_2} increases linearly up to a p_{CO} of 1.0 atm, after which it plateaus at approximately 90 mmol g_x^{-1} h^{-1}. This might indicate that the microorganism metabolized CO at near-maximal rates at a pCO > 1.0 atm. Up to a p_{CO} of 0.45, trace amounts of hydrogen were measured in the

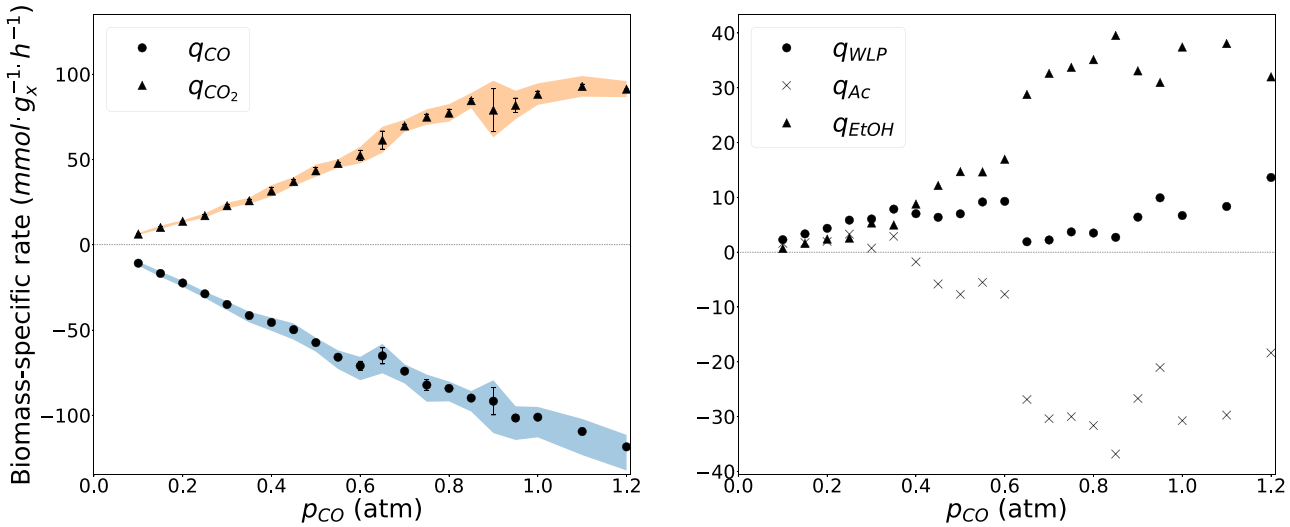

FIGURE 1 Biomass-specific fluxes during CO pulses. Left panel: CO uptake rate (q_{CO}) and CO_2 production rate (q_{CO_2}) as a function of the fraction of CO in the inlet gas. The biomass-specific rates were determined from two, three, or four individual biological replicates, and the error bars depict the standard deviation. The shaded area shows the error range of the calculated rates based on the standard deviation in the steady-state biomass concentration and the standard deviations. Right panel: Flux distribution analysis illustrating the relationship between CO partial pressure, the rate through central carbon metabolism (q_{WLP}) and the production rates of acetate (q_{Ac}) and ethanol (q_{EtOH}). The rates were calculated using q_{co} and q_{co_2}, considering that all carbon and electrons consumed by *C. autoethanogenum* must be recovered in the products and that oxidation and reduction of redox carriers in the metabolism must be balanced. Negative values for a biomass-specific rate indicate net consumption of a metabolite.

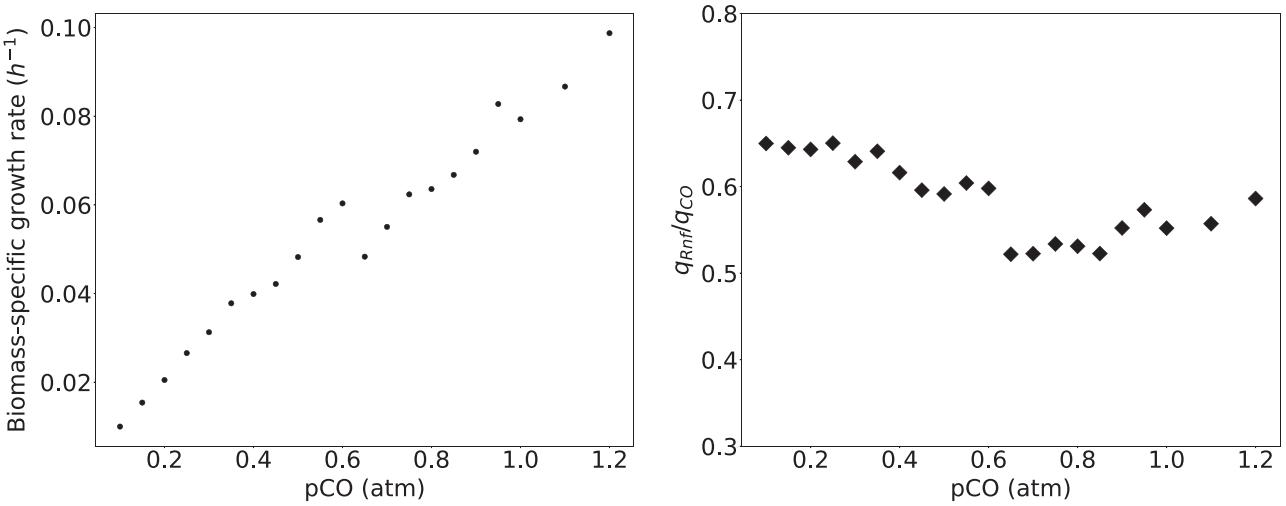

FIGURE 2 Estimated biomass-specific growth rate (μ, left) and the flux of the Rnf complex (q_{Rnf}) divided by the observed q_{CO} (right). The biomass-specific growth rate was estimated by using q_{Rnf} and the stoichiometries of the Rnf and ATPase complexes shown in Figure 1 to calculate the biomass-specific ATP production rate. The ATP production rate was multiplied by the biomass yield on ATP (Y_{ATP}) derived from steady-state data to obtain the biomass-specific growth rate. q_{Rnf}/q_{CO} gives a proxy for the ATP yield per mol of CO consumed.

reactor off-gas, but the biomass-specific hydrogen production rate decreased with increasing p_{CO} (Supporting Information: Figure S3). The differences between the q_{CO} and q_{CO_2} profiles could be accounted for by changes in metabolic strategy (Figure 1).

3.3 | Acetate consumption for sustaining increased q_{CO} leads to shifts in product spectrum

The effect of increasing CO uptake rates on the metabolism of *C. autoethanogenum* was assessed with a stoichiometric model of the central carbon metabolism. The measured q_{CO}, q_{CO_2}, and q_{H_2} were used as input values to calculate the fluxes of product formation and the flux through the WLP, as shown in Figure 1 (right panel). A shift was observed from the formation of mainly acetate at a p_{CO} of 0.1–0.35 atm to the formation of mainly ethanol until a p_{CO} of 0.6 atm. Above pCO of 0.6 atm a net consumption of acetate for additional ethanol production was observed. The flux distribution analysis based on off-gas data was cross-verified with measurements of pH and metabolites in the culture broth (Supporting Information: Figure S4), confirming that shifts in the catabolic strategy of *C. autoethanogenum* can be identified based solely on off-gas measurements. Notably, the overall rate through the WLP did not increase proportionally with increasing q_{CO}. The highest observed q_{WLP} was 13.6 mmol g_x^{-1} h^{-1}.

Estimated growth rates, q_{Rnf}, and q_{CO} during the pulse experiments were analyzed to investigate the effect of shifts in the product spectrum on the energy conservation of *C. autoethanogenum*. The biomass yield on ATP (Y_{ATP}) was calculated from chemostat data (Table 2) and equaled 2.6 g_x per mol ATP. The biomass-specific ATP production rate (q_{ATP}) during the pulse experiments was calculated by multiplying q_{Rnf}, following from the flux distribution analysis, with the assumed H^+/ATP stoichiometry of *C. autoethanogenum* (Supporting Information: Figure S6). The growth rate (μ) was calculated assuming that Y_{ATP} is equal in chemostat and pulse conditions, following $\mu = Y_{ATP} \cdot q_{ATP}$, and was found to increase linearly with increasing p_{CO} (Figure 2, left panel). The activity of the Rnf complex and the membrane-bound ATPase is the only source for net ATP production in *C. autoethanogenum* when growing on CO (as the WLP is ATP neutral) (Supporting Information: Figure S6). Therefore, the rate of the Rnf complex relative to the CO uptake rate is a proxy for the ATP yield on CO during the pulse experiments and decreased with an increasing flux towards ethanol (Figure 2).

4 | DISCUSSION

This study aimed to identify q_{CO}^{max} of *C. autoethanogenum* by using dynamic CO-feeding experiments. 1-h pulses were administered to a steady-state chemostat culture, gradually increasing the p_{CO} up to 1.2 atm. By increasing the fraction of CO in the inlet gas and the headspace pressure while maintaining a constant overall inlet gas flow rate, the mass transfer rate in the system was effectively enhanced without affecting the k_La. A similar approach was employed by Novak et al. (2021) to determine q_{H_2} of *Acetobacterium woodii*, though in that case, higher stirring speeds were used to obtain a new steady state at an increased mass transfer capacity in a H_2/CO_2-fed system. The advantage of the method used in our study is that the k_La remains constant, and the pulse experiments have a short duration, allowing the system to return to steady state rapidly. These characteristics facilitate the performance of multiple biological replicates and save time compared to obtaining different steady-state datasets.

In a gas-fed bioreactor, the mass transfer or biological conversion rate limits the substrate conversion rate. When the latter is the case,

the substrate concentration in the liquid will build up. So far, it has been widely accepted that the build-up of CO in the liquid can lead to metabolic arrest, with CO inhibition constants around 0.1 mM (Ruggiero et al., 2022). This occurs because CO binds to the active site of metalloenzymes, rendering them inactive (Menon & Ragsdale, 1996; Schuchmann et al., 2018). Various enzymes involved in the WLP rely on metal clusters. Consequently, a decrease in metabolic activity due to CO toxicity would result in reduced CO uptake rates, resulting in noticeable changes in the off-gas profile. These observations would indicate that the limit of the biomass-specific CO uptake rate (q_{CO}^{max}) has been reached. Interestingly, in our experiments, q_{CO} continued to increase over the entire range of CO partial pressures, up to -119 ± 1 mmol g_x^{-1} h^{-1}. This high biological capacity for CO conversion by *C. autoethanogenum* was not exhibited at lower p_{CO}, which could either be due to low affinity for CO or due to mass transfer limitation in the bioreactor system. The study by Mann et al. (2021) showed high CO affinity by *C. ljungdahlii*, which is able to bring the dissolved CO tension close to zero during continuous cultivation. Given the >99% genetic resemblance (Utturkar et al., 2015) and highly similar physiological characteristics of *C. autoethanogenum* and *C. ljungdahlii*, it is likely that *C. autoethanogenum* also has high CO affinity. Furthermore, the actual CO concentration in the liquid must have been below the inhibition constant for CO, as we observed no apparent decrease in the metabolic capacity in our experiments. Therefore, the linear relation between the measured q_{CO} and the CO supply rate suggests that the liquid CO concentration increased only marginally (i.e., sufficiently to sustain a higher rate). Our data, therefore, suggests that the biological conversion of CO was mass transfer limited over the entire range of tested p_{CO}. Future dynamic bioreactor work combining dissolved CO measurements with off-gas analysis could further resolve the inhibition kinetics of CO.

In this study, we could not identify q_{CO}^{max} of *C. autoethanogenum* in our bioreactor system. This contrasts with previous studies with *C. ljungdahlii*, where a metabolic collapse occurred due to CO accumulation in the liquid at a q_{CO} of −42 mmol g_x^{-1} h^{-1} (Mann et al., 2021). In their study, high mass transfer rates were maintained longer than in the experiments performed here. This shows that the time of exposure to elevated p_{CO} could also affect microbial survival rates. Conducting CO pulse experiments of varying durations could provide valuable insights into the CO consumption capacity of *C. autoethanogenum* and warrant an exciting avenue for further investigation.

Our study proves the need for dedicated and well-controlled experimental validation of critical kinetic parameters. It shows that the CO uptake capacity of *C. autoethanogenum* has been severely underestimated to date. The highest observed q_{CO} in this study is 2.5–3.5-fold higher than the q_{CO}^{max} reported in kinetic modeling studies that used only steady-state chemostat or batch bottle data for parameter estimation and 1.8-fold higher than the highest q_{CO} reported in the literature for *C. autoethanogenum* (de Lima et al., 2022; de Medeiros et al., 2019; Mohammadi et al., 2014). Furthermore, verifying whether mass transfer or biological capacity limited the CO conversion rate in previous studies is impossible. Our study shows that mass transfer limitation in the model systems likely leads to the prediction of lower values for q_{CO}^{max} than the q_{CO} of -119 ± 1 mmol g_x^{-1} h^{-1} observed here. To improve the predictive power of kinetic models further, obtaining the actual q_{CO}^{max} of *C. autoethanogenum* is pivotal. Bioreactor systems with a different geometry or impeller type could be helpful, as increased stirring rates also increase the mass transfer capacity of a bioreactor system (de Lima et al., 2022; Hermann et al., 2020; Mann et al., 2021; Novak et al., 2021; Valgepea et al., 2017). Higher stirring speeds in the bioreactor system used here led to vortex formation around the impellers, which was detrimental to the mass transfer rate (Supporting Information: Figure S5). Alternatively, a pressurizable bioreactor system could be employed to increase p_{CO} further and investigate its impact on q_{CO}, or higher q_{CO} could be achieved in a system operated at a lower biomass concentration.

When interpreting the results of this study, it should be considered that the bioreactor has been operated for five months (including a one-month recovery after a technical disturbance) under the pulse-feeding regime. Therefore, it cannot be completely excluded that the culture has adapted to fluctuating conditions. For example, enzyme levels could be regulated to increase the cellular CO uptake capacity, or alterations could be made to the cell wall structure to reduce the permeability of CO. However, adjustments in the proteome are unlikely, as previous work has shown that protein expression did not change even in chemostat experiments where periodically highly fluctuating CO and H_2 uptake rates were observed (Mahamkali et al., 2020). Still, phenotype-altering mutations might accumulate in the genome during long-term exposure to fluctuating conditions (Ingelman et al., 2023). It can, however, be argued that strains with such mutations resemble industrial workhorses since microorganisms continuously experience fluctuating conditions in industrial-scale systems (Puiman et al., 2023).

The combination of online off-gas measurements and flux distribution analysis provides a powerful means to monitor product distribution during CO fermentation without liquid measurements. This approach highlights the effectiveness of dynamic bioreactor experiments with online data analysis for studying microbial physiology, as also demonstrated earlier by Allaart et al. (2021) and Stouten et al. (2021). However, careful experimental design is pivotal to extracting the desired information from the experimental data. In our study, we observed that acetate was the main catabolic product for pulses up to a p_{CO} of 0.35. However, as the p_{CO} increased, more ethanol was formed at the expense of acetate in the fermentation broth. This shift from net acetate production to net acetate consumption is noteworthy. Similar observations have been made in *C. autoethanogenum* and other closely related *Clostridium* species (de Lima et al., 2022; Hurst & Lewis, 2010; Mann et al., 2021; Phillips et al., 2015). The observed changes in physiology align with the overflow hypothesis of Allaart et al. (2023), stating that acetate reduction to ethanol is exploited to mitigate CO toxicity.

In the experiments performed here, we controlled the rate at which CO was supplied via the mass transfer rate. Through metabolic flux analysis, we observed that the flux through the WLP did not increase significantly beyond a p_{CO} of 0.6 atm. However, the increased CO uptake rate was compensated with higher rates of acetate reduction to ethanol. This is likely to be related to the redox state of the electron carriers and the fact that acetate was available in the cultivation broth (Diender et al., 2019; Mahamkali et al., 2020; Richter et al., 2016; Schulz et al., 2023; Xu et al., 2020). Effectively, the product spectrum changed as a function of the mass transfer rate. In other words, the product spectrum of CO fermentation can be controlled by controlling the CO uptake rate through the operational conditions of the bioreactor. This provides an appealing alternative to tedious genetic engineering strategies for improving ethanol production from CO-containing waste.

NOMENCLATURE

N	amount of a gaseous species (mol)
M	amount of a dissolved species (mol)
F	gas- or liquid flow (mol h^{-1})
y	gas fraction (−)
C	concentration (mol L^{-1})
T	gas/liquid transfer term (mol h^{-1})
V	volume (L)
v	flux (mmol h^{-1})
q	biomass-specific rate (mmol $g_x^{-1}h^{-1}$)

SUBSCRIPTS

G	gas (−)
L	liquid (−)
in	inflowing (−)
out	outflowing (−)
CO	carbon monoxide gas (−)
N_2	nitrogen gas (−)
H_2	hydrogen gas (−)
CO_2	carbon dioxide, sum of gaseous and dissolved species (−)
i	Species 'i' (−)
x	biomass (−)
Ac	acetate (−)
EtOH	ethanol (−)
CODH	carbon monoxide dehydrogenase (−)
MTHFR	methylene tetrahydrofolate reductase (−)
Rnf	*Rhodobacter* nitrogen fixation enzyme complex (−)
AOR	acetaldehyde oxidoreductase (−)
Nfn	electron confurcating complex (−)
FDH	formate dehydrogenase (−)
CODH/ACS	carbon monoxide dehydrogenase/acetyl-CoA synthase complex (−)
ALDH	acetaldehyde dehydrogenase (−)
ADH	alcohol dehydrogenase (−)
MTHFD	methylene tetrahydrofolate dehydrogenase (−)
ACK	acetate kinase enzyme (−)

AUTHOR CONTRIBUTIONS

Maximilienne T. Allaart: Conceptualization; methodology; formal analysis; investigation, writing—original draft; review and editing. **Charilaos Korkontzelos**: Investigation; formal analysis. **Diana Z. Sousa**: Conceptualization; resources; supervision; writing—review and editing. **Robbert Kleerebezem**: Conceptualization; methodology; supervision; resources; writing—review and editing.

ACKNOWLEDGMENTS

The authors would like to thank Martijn Diender for valuable discussions about the experiments and Marina Elisiário for her help with reactor operation. This publication is part of project 3 of the Perspectief Programma MicorSynC (P16-10), which is (partly) financed by the Domain Applied and Engineering Sciences (AES) from the Dutch Research Council (NWO).

CONFLICT OF INTEREST STATEMENT

The authors declare no conflict of interest.

DATA AVAILABILITY STATEMENT

The data that support the findings of this study are openly available in 4TU Research Database at https://data.4tu.nl/private_datasets/6gzFKW_nNWmOXB0eypwsUGa6YTm1LNpIYaV7BFrx5XQ The authors confirm that the data supporting the findings of this study are available within the article and its supplementary materials.

ETHICS STATEMENT

This article does not contain any studies with human participants or animals performed by any of the authors.

ORCID

Maximilienne T. Allaart http://orcid.org/0000-0002-9711-3954

REFERENCES

Abrini, J., Naveau, H., & Nyns, E. J. (1994). *Clostridium autoethanogenum*, sp. nov., an anaerobic bacterium that produces ethanol from carbon monoxide. *Archives of Microbiology*, *161*, 345–351.

Ahmed, A., & Lewis, R. S. (2007). Fermentation of biomass-generated synthesis gas: Effects of nitric oxide. *Biotechnology and Bioengineering*, *97*(5), 1080–1086. https://doi.org/10.1002/bit.21305

Allaart, M. T., Diender, M., Sousa, D. Z., & Kleerebezem, R. (2023). Overflow metabolism at the thermodynamic limit of life: How carboxydotrophic acetogens mitigate carbon monoxide toxicity. *Microbial Biotechnology*, *16*, 697–705. https://doi.org/10.1111/1751-7915.14212

Allaart, M. T., Stouten, G. R., Sousa, D. Z., & Kleerebezem, R. (2021). Product inhibition and pH affect stoichiometry and kinetics of chain elongating microbial communities in sequencing batch bioreactors. *Frontiers in Bioengineering and Biotechnology*, *9*(June), 693030. https://doi.org/10.3389/fbioe.2021.693030

APHA/AWWA/WEF. (1999). *Standard methods for the examination of water and wastewater*. Standard Methods.

Arantes, A. L., Moreira, J., Diender, M., Parshina, S. N., Stams, A., Alves, M. M., Alves, J. I., & Sousa, D. Z. (2020). Enrichment of anaerobic syngas-converting communities and isolation of a novel carboxydotrophic *Acetobacterium wieringae* strain JM. *Frontiers in*

Microbiology, *11*(January), 58. https://doi.org/10.3389/fmicb.2020.00058

Arena, U. (2012). Process and technological aspects of municipal solid waste gasification. A review. *Waste Management*, *32*(4), 625–639. https://doi.org/10.1016/j.wasman.2011.09.025

Cotter, J. L., Chinn, M. S., & Grunden, A. M. (2009). Influence of process parameters on growth of *Clostridium ljungdahlii* and *Clostridium autoethanogenum* on synthesis gas. *Enzyme and Microbial Technology*, *44*(5), 281–288. https://doi.org/10.1016/j.enzmictec.2008.11.002

Diender, M., Parera Olm, I., Gelderloos, M., Koehorst, J. J., Schaap, P. J., Stams, A., & Sousa, D. Z. (2019). Metabolic shift induced by synthetic co-cultivation promotes high yield of chain elongated acids from syngas. *Scientific Reports*, *9*, 18081. https://doi.org/10.1038/s41598-019-54445-y

Dry, M. E. (2002). The Fischer-Tropsch process: 1950-2000. *Catalysis Today*, *71*(3–4), 227–241. https://doi.org/10.1016/S0920-5861(01)00453-9

Heffernan, J. K., Mahamkali, V., Valgepea, K., Marcellin, E., & Nielsen, L. K. (2022). Analytical tools for unravelling the metabolism of gas-fermenting *Clostridia*. *Current Opinion in Biotechnology*, *75*(Table 1), 102700. https://doi.org/10.1016/j.copbio.2022.102700

Heffernan, J. K., Valgepea, K., de Souza Pinto Lemgruber, R., Casini, I., Plan, M., Tappel, R., Simpson, S. D., Köpke, M., Nielsen, L. K., & Marcellin, E. (2020). Enhancing CO2-valorization using *Clostridium autoethanogenum* for sustainable fuel and chemicals production. *Frontiers in Bioengineering and Biotechnology*, *8*(March), 204. https://doi.org/10.3389/fbioe.2020.00204

Hermann, M., Teleki, A., Weitz, S., Niess, A., Freund, A., Bengelsdorf, F. R., & Takors, R. (2020). Electron availability in CO_2, CO and H_2 mixtures constrains flux distribution, energy management and product formation in *Clostridium ljungdahlii*. *Microbial Biotechnology*, *13*(6), 1831–1846. https://doi.org/10.1111/1751-7915.13625

Hurst, K. M., & Lewis, R. S. (2010). Carbon monoxide partial pressure effects on the metabolic process of syngas fermentation. *Biochemical Engineering Journal*, *48*(2), 159–165. https://doi.org/10.1016/j.bej.2009.09.004

IEA. (2020). Iron and steel technology roadmap. In *Iron and Steel Technology Roadmap*. https://doi.org/10.1787/3dcc2a1b-en

Ingelman, H., Heffernan, J. K., Harris, A., Brown, S. D., Saqib, A. Y., Pinheiro, M. J., Lima, L. A., de Martinez, K. R., Gonzalez-Garcia, R. A., Hawkins, G., Daleiden, J., Tran, L., Zeleznik, H., Jensen, R. O., Reynoso, V., Simpson, S. D., Köpke, M., Marcellin, E., & Valgepea, K. (2023). Autotrophic adaptive laboratory evolution of the acetogen *Clostridium autoethanogenum* delivers the gas-fermenting strain LAbrini with superior growth, products, and robustness. *BioRxiv*. Advance published online. https://doi.org/10.1101/2023.01.28.526018

Klask, C. M., Kliem-Kuster, N., Molitor, B., & Angenent, L. T. (2020). Nitrate feed improves growth and ethanol production of *Clostridium ljungdahlii* with CO_2 and H_2, but results in stochastic inhibition events. *Frontiers in Microbiology*, *11*(May), 724. https://doi.org/10.3389/fmicb.2020.00724

Lee, J., Lee, J. W., Chae, C. G., Kwon, S. J., Kim, Y. J., Lee, J. H., & Lee, H. S. (2019). Domestication of the novel alcohologenic acetogen *Clostridium* sp. AWRP: From isolation to characterization for syngas fermentation. *Biotechnology for Biofuels*, *12*(1), 228. https://doi.org/10.1186/s13068-019-1570-0

Levy, P. F., Barnard, G. W., Garcia-Martinez, D. V., Sanderson, J. E., & Wise, D. L. (1981). Organic acid production from CO_2/H_2 and CO/H_2 by mixed-culture anaerobes. *Biotechnology and Bioengineering*, *23*(10), 2293–2306. https://doi.org/10.1002/bit.260231012

de Lima, L. A., Ingelman, H., Brahmbhatt, K., Reinmets, K., Barry, C., Harris, A., Marcellin, E., Köpke, M., & Valgepea, K. (2022). Faster growth enhances low carbon fuel and chemical production through gas fermentation. *Frontiers in Bioengineering and Biotechnology*, *10*(April), 879578. https://doi.org/10.3389/fbioe.2022.879578

Mahamkali, V., Valgepea, K., de Souza Pinto Lemgruber, R., Plan, M., Tappel, R., Köpke, M., Simpson, S. D., Nielsen, L. K., & Marcellin, E. (2020). Redox controls metabolic robustness in the gas-fermenting acetogen *Clostridium autoethanogenum*. *Proceedings of the National Academy of Sciences of the United States of America*, *117*(23), 13168–13175. https://doi.org/10.1073/pnas.1919531117

Mann, M., Miebach, K., & Büchs, J. (2021). Online measurement of dissolved carbon monoxide concentrations reveals critical operating conditions in gas fermentation experiments. *Biotechnology and Bioengineering*, *118*(1), 253–264. https://doi.org/10.1002/bit.27567

de Medeiros, E. M., Posada, J. A., Noorman, H., & Filho, R. M. (2019). Dynamic modeling of syngas fermentation in a continuous stirred-tank reactor: Multi-response parameter estimation and process optimization. *Biotechnology and Bioengineering*, *116*(10), 2473–2487. https://doi.org/10.1002/bit.27108

Menon, S., & Ragsdale, S. W. (1996). Unleashing hydrogenase activity in carbon monoxide dehydrogenase/acetyl-CoA synthase and pyruvate:ferredoxin oxidoreductase. *Biochemistry*, *35*(49), 15814–15821. https://doi.org/10.1021/bi9615598

Mohammadi, M., Mohamed, A. R., Najafpour, G. D., Younesi, H., & Uzir, M. H. (2014). Kinetic studies on fermentative production of biofuel from synthesis gas using *Clostridium ljungdahlii*. *The Scientific World Journal*, *2014*, 1–8. https://doi.org/10.1155/2014/910590

Molitor, B., Richter, H., Martin, M. E., Jensen, R. O., Juminaga, A., Mihalcea, C., & Angenent, L. T. (2016). Carbon recovery by fermentation of CO-rich off gases - Turning steel mills into biorefineries. *Bioresource Technology*, *215*, 386–396. https://doi.org/10.1016/j.biortech.2016.03.094

Novak, K., Neuendorf, C. S., Kofler, I., Kieberger, N., Klamt, S., & Pflügl, S. (2021). Blending industrial blast furnace gas with H2 enables *Acetobacterium woodii* to efficiently co-utilize CO, CO_2 and H_2. *Bioresource Technology*, *323*(124573), 124573. https://doi.org/10.1016/j.biortech.2020.124573

Phillips, J. R., Atiyeh, H. K., Tanner, R. S., Torres, J. R., Saxena, J., Wilkins, M. R., & Huhnke, R. L. (2015). Butanol and hexanol production in *Clostridium carboxidivorans* syngas fermentation: Medium development and culture techniques. *Bioresource Technology*, *190*, 114–121. https://doi.org/10.1016/j.biortech.2015.04.043

Puiman, L., Almeida Benalcázar, E., Picioreanu, C., Noorman, H. J., & Haringa, C. (2023). Downscaling industrial-scale syngas fermentation to simulate frequent and irregular dissolved gas concentration shocks. *Bioengineering*, *10*(518), 518.

Puiman, L., Elisiário, M. P., Crasborn, L. M. L., Wagenaar, L. E. C. H., Straathof, A. J. J., & Haringa, C. (2022). Gas mass transfer in syngas fermentation broths is enhanced by ethanol. *Biochemical Engineering Journal*, *185*(June), 108505. https://doi.org/10.1016/j.bej.2022.108505

Richter, H., Molitor, B., Wei, H., Chen, W., Aristilde, L., & Angenent, L. T. (2016). Ethanol production in syngas-fermenting: *Clostridium ljungdahlii* is controlled by thermodynamics rather than by enzyme expression. *Energy & Environmental Science*, *9*(7), 2392–2399. https://doi.org/10.1039/c6ee01108j

Rückel, A., Hannemann, J., Maierhofer, C., Fuchs, A., & Weuster-Botz, D. (2021). Studies on syngas fermentation with *Clostridium carboxidivorans* in stirred-tank reactors with defined gas impurities. *Frontiers in Microbiology*, *12*(April), 655390. https://doi.org/10.3389/fmicb.2021.655390

Ruggiero, G., Lanzillo, F., Raganati, F., Russo, M. E., Salatino, P., & Marzocchella, A. (2022). Bioreactor modelling for syngas fermentation: Kinetic characterization. *Food and Bioproducts Processing*, *134*, 1–18. https://doi.org/10.1016/j.fbp.2022.04.002

Schuchmann, K., Chowdhury, N. P., & Müller, V. (2018). Complex multimeric [FeFe] hydrogenases: Biochemistry, physiology and new opportunities for the hydrogen economy. *Frontiers in Microbiology*, *9*(DEC), 2911. https://doi.org/10.3389/fmicb.2018.02911

Schulz, S., Molitor, B., & Angenent, L. T. (2023). Acetate augmentation boosts the ethanol production rate and specificity by *Clostridium ljungdahlii* during gas fermentation with pure carbon monoxide. *Bioresource Technology*, *369*(128387), 128387. https://doi.org/10.1016/j.biortech.2022.128387

Sipkema, E. M., De Koning, W., Ganzeveld, K. J., Janssen, D. B., & Beenackers, A. A. C. M. (1998). Experimental pulse technique for the study of microbial kinetics in continuous culture. *Journal of Biotechnology*, *64*(2–3), 159–176. https://doi.org/10.1016/S0168-1656(98)00076-5

Stouten, G. R., Douwenga, S., Hogendoorn, C., & Kleerebezem, R. (2021). System characterization of dynamic biological systems through improved data analysis. *BioRxiv*, *1*, 1–17.

Stouthamer, A. H., & Bettenhaussen, C. (1973). Utilization of energy for growth and maintenance in continuous and batch cultures of microorganisms. *Biochimica et Biophysica Acta (BBA) - Reviews on Bioenergetics*, *301*(1), 53–70. https://doi.org/10.1016/0304-4173(73)90012-8

Utturkar, S. M., Klingeman, D. M., Bruno-Barcena, J. M., Chinn, M. S., Grunden, A. M., Köpke, M., & Brown, S. D. (2015). Sequence data for *Clostridium autoethanogenum* using three generations of sequencing technologies. *Scientific Data*, *2*, 150014. https://doi.org/10.1038/sdata.2015.14

Valgepea, K., De Souza Pinto Lemgruber, R., Abdalla, T., Binos, S., Takemori, N., Takemori, A., Tanaka, Y., Tappel, R., Köpke, M., Simpson, S. D., Nielsen, L. K., & Marcellin, E. (2018). H_2 drives metabolic rearrangements in gas-fermenting *Clostridium autoethanogenum*. *Biotechnology for Biofuels*, *11*(1), 55. https://doi.org/10.1186/s13068-018-1052-9

Valgepea, K., de Souza Pinto Lemgruber, R., Meaghan, K., Palfreyman, R. W., Abdalla, T., Heijstra, B. D., Behrendorff, J. B., Tappel, R., Köpke, M., Simpson, S. D., Nielsen, L. K., & Marcellin, E. (2017). Maintenance of ATP homeostasis triggers metabolic shifts in gas-fermenting acetogens. *Cell Systems*, *4*(5), 505–515.e5.e5. https://doi.org/10.1016/j.cels.2017.04.008

Wett, B., Schoen, M., Phothilangka, P., Wackerle, F., & Insam, H. (2007). Model-based design of an agricultural biogas plant: Application of anaerobic digestion model no. 1 for an improved four chamber scheme. *Water Science and Technology*, *55*(10), 21–28. https://doi.org/10.2166/wst.2007.302

World Steel Organization. (2022). *World steel in figures* (Vol. 2003). WSO. http://www.worldsteel.org/wsif.php

Xu, H., Liang, C., Chen, X., Xu, J., Yu, Q., Zhang, Y., & Yuan, Z. (2020). Impact of exogenous acetate on ethanol formation and gene transcription for key enzymes in *Clostridium autoethanogenum* grown on CO. *Biochemical Engineering Journal*, *155*(June 2019), 107470. https://doi.org/10.1016/j.bej.2019.107470

SUPPORTING INFORMATION

Additional supporting information can be found online in the Supporting Information section at the end of this article.

How to cite this article: Allaart, M. T., Korkontzelos, C., Sousa, D. Z., & Kleerebezem, R. (2024). A novel experimental method to determine substrate uptake kinetics of gaseous substrates applied to the carbon monoxide-fermenting *Clostridium autoethanogenum*. *Biotechnology and Bioengineering*, *121*, 1324–1334. https://doi.org/10.1002/bit.28652